ELSEVIER

Journal of Molecular Structure 508 (1999) 87–96

Journal of
MOLECULAR
STRUCTURE

Comparison between the polarized Fourier-transform infrared spectra of aged porous silicon and amorphous silicon dioxide films on Si (100) surface

Jianping Wang, Bingsuo Zou, Mostafa A. El-Sayed*

Laser Dynamics Laboratory, School of Chemistry and Biochemistry, Georgia Institute of Technology, Atlanta, GA 30332-0400, USA

Received 13 November 1998; accepted 22 December 1998

Abstract

The s- and p-polarized Fourier transform infrared spectra were measured for an aged porous silicon (PS) film on Si (100) surface. The asymmetric stretching and symmetric stretching modes as well as the bending or rocking mode of the Si–O–Si group are studied. The deconvoluted spectra in Si–O–Si asymmetric stretching frequency region at different polarization directions show two pairs of vibrational modes, and can be assigned to the longitudinal-optic (LO) and transverse-optic (TO) pair of the corresponding vibrational modes. The smaller LO–TO pair splitting, the broader bandwidth, and the lower polarization ratio of the PS vibration bands as compared with those observed in an a-SiO_2 film on Si wafer, suggest a less ordered SiO_2 structure and a shorter range of coulombic interaction in PS.

Keywords: Porous silicon; Amorphous SiO_2; Polarized FTIR; LO–TO splitting

1. Introduction

Porous silicon (PS) formed by electrochemical anodization yields visible photoluminescence (PL) with high quantum efficiency at room temperature [1]. Extensive studies were carried out in the last few years, aiming to understand the origin of the PL and explore the potential applications of this luminescence in Si-based optoelectronic devices [2].

Vibrational spectroscopy is an important technique for identifying the molecular species on the PS surface, and studying the possible roles of those species in the PL. It was also suggested that surface chemistry play an important role in producing the species giving rise to the visible PL of PS, because as-prepared and annealed PS films give different peak positions in the PL spectra as well as different absorption bands in the IR spectra [3]. In a previous study [4], a correlation between surface chemistry and PL peak wavelength was suggested, based on the finding that the luminescence peak frequency shifts to the blue region with increasing Si–O/Si–H IR absorption band ratio. A broad IR band at around 1100 cm^{-1} grows as PS ages in air [5], or after anodic oxidation [6]. Annealed siloxene ($Si_6O_3H_6$) and oxidized PS give similar IR spectra, and therefore a possible common luminescence mechanism in these two materials was suggested [7–9]. The decrease of the OH IR

* Corresponding author. Tel.: +1-404-894-0292; fax: +1-404-894-0294.

E-mail address: mostafa.el-sayed@chemistry.gatech.edu (A. El-Sayed)

0022-2860/99/$ - see front matter
PII: S0022-2860(99)00003-4

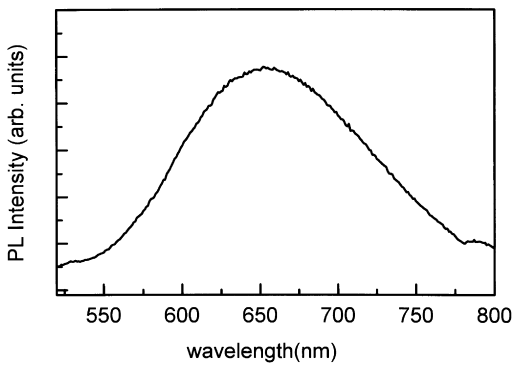

Fig. 1. The photoluminescence spectrum of the PS. Excitation at 355 nm, at room temperature.

band is associated with the luminescence activation process, as monitored using in situ luminescence and IR study [10]. Recently Mawhinney et al. [11] studied the oxidation of a hydrogen-terminated PS surface by transmission FTIR spectroscopy. Evidence was given for the formation of three surface species after oxidation: Si–O–Si (having a broad band at 1100 cm^{-1}), $-O_ySiH_x$ (having a weak band at 2276 cm^{-1}), and SiO–H (having a weak band at 3376 cm^{-1}). Gole et al. [12] suggested a reassignment of a portion of the 1176 cm^{-1} band in the 1300–1100 cm^{-1} region to the Si=O stretching mode of the silanone-based oxyhdrides, based on their quantum chemical calculation [13].

Silicon hydride terminated PS (as-prepared) may change to silicon oxide terminated and become stabilized either by thermal oxidation or prolonged aging in air (natural oxidation). Oxidized PS has crystalline Si (c-Si) in the core and SiO_x ($x = 1, 2$) on the surface [14]. The vibrations of the silicon–oxygen bonds in the oxidized PS can thus be characterized by comparison with its analog, a-SiO_2.

In this paper, the longitudinal-optic (LO)–transverse-optic (TO) vibrational modes of an aged PS film (and of an a-SiO_2 film) are observed by use of polarized FTIR spectroscopy in the region 400–1400 cm^{-1}, and compared with those previously reported [15–17] for a-SiO_2. The smaller LO–TO pair splitting, the broader bandwidth, and the smaller polarization ratios of the vibrational bands in PS, are proposed to be the manifestation of a less ordered Si–O–Si structure with short-range interaction on the surface of the PS nanostructure.

2. Experimental

2.1. Materials

The p-type, boron-doped, 2–5 Ω cm, (100)-oriented Si wafers were rinsed in aqueous HNO_3 (30 min) for surface cleaning and then rinsed thoroughly in doubly de-ionized water (DDW) before use. The PS samples were prepared by electrochemical etching [18]. Aluminum film was deposited on the back of the samples to improve the uniformity of the anodic current during the etch process. The electrolyte is a 1 : 1 mixture of 1 : 1 (volume) methanol and concentrated aqueous HF (48%). Anodization was carried out using 20 mA/cm^2 for 15–20 min. After etching, the silicon surface was rinsed with DDW. The PS layer (typically 2–5 μm thick) exhibited intense orange PL to the naked eye under 365 nm UV light irradiation. Oxidized PS wafers were obtained by aging in air for two weeks.

The a-SiO_2 wafers were prepared by thermal oxidization in a tube furnace in an oxygen environment. The clean Si wafers were put into a preheated (800°C) oxygen furnace and ramped up to 1000°C within 20 min. The wafers were oxidized on both sides at 1000°C for 1 h before cooling them to 800°C and then further cooling them to room temperature in the absence of oxygen. No orange or red photoluminescence was observed for these a-SiO_2 films.

2.2. Luminescence spectrum

The emission spectrum was measured using a fluorescence spectrometer (PTi, Photon Technology International), with excitation wavelength at 355 nm. The emission spectrum of PS is shown in Fig. 1. This spectrum and the emission decay time of our oxidized PS samples are found to have the similar characteristics with those reported previously [19].

2.3. Polarized FTIR spectroscopy

A Bruker IFS66/S FTIR spectrometer is used, with a liquid-nitrogen-cooled photovoltaic mercury–cadmium–telluride (MCT) detector (Kolmar technologies Inc., KMPV11-1-LJ2) for the mid-IR region. A polarized IR incident beam is obtained using a wire-grid polarizer (Graseby 12000 series). All spectra were the average of 100 scans at a resolution of

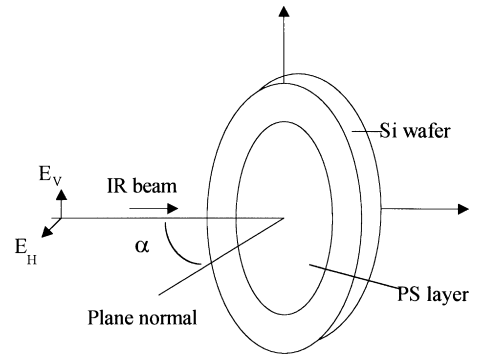

Fig. 2. A diagram of the experimental geometrical arrangement showing the oblique incident radiation direction with respect to the sample plane normal: perpendicular (E_V, s-polarized) and parallel (E_H, p-polarized). An oblique angle α (60°–70°) is used to generate p-polarization. The IR beam is in the plane of paper. The silicon wafer surface is tilted with an angle α between its normal and the IR beam.

2 cm^{-1}. Spectral subtraction between the spectrum for PS or a-SiO_2 and that for a bare silicon wafer was performed to remove the major absorption band at $\sim$ 610 cm^{-1} and other band features of crystalline silicon.

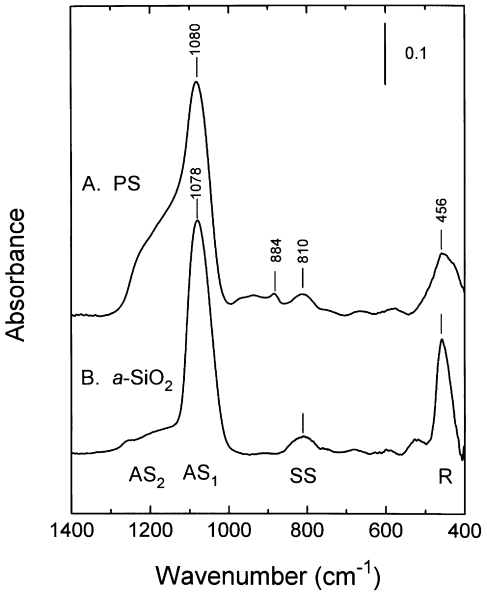

Fig. 3. The s-polarized FTIR spectra of oxidized PS layer (A) and a-SiO_2 layer (B) on Si (100) in 400–1400 cm^{-1}. The bare silicon wafer absorption bands at 1106 and 610 cm^{-1} was subtracted from these spectra.

Fig. 2 shows a sketch of the experimental arrangement used in the polarized FTIR spectra measurements. The definition of the s- and p-polarization is also given in this figure. Experimentally, an oblique angle α (60°–70°, the angle between the IR beam and the normal to the sample plane) is used to obtain p-polarization. For the p-polarization, the electric field of the IR beam has a large vector perpendicular to the sample surface (at $\alpha = 60°–70°$), whereas for the s-polarization, this vector is parallel to the sample surface plane ($\alpha = 0°$). As p-polarization has significant electric field vector intensity along the Si wafer plane as well as perpendicular to it, p-polarized spectra contain both TO and LO modes whereas s-polarized spectra contain mostly TO modes.

Curve fitting was carried out using the local-least-squares algorithm under the OPUS 2.0 software provided for the Bruker FTIR spectrometer. A Gaussian band shape was chosen for each decomposed absorption component except where otherwise mentioned. The root mean square (RMS) error was minimized for the optimized fitted results. An optimized fitting consists of the minimum number of band components that are physically meaningful when fitting both the band shape and bandwidth.

3. Results

3.1. FTIR spectra of PS and surface oxidized a-SiO_2

Fig. 3 shows the s-polarized FTIR spectra, in the 1400–400 cm^{-1} region, for an oxidized PS (curve A) and a-SiO_2 film (curve B). For PS, there are four major bands. The broad band at 1300–1000 cm^{-1} (with peak at 1080 cm^{-1}) is assigned to the asymmetric stretching (AS) mode of the Si–O–Si moiety. As shown in the next section, this mode contains two components [16], namely an AS_1 mode (in-phase motion of two adjacent oxygen atoms with respect to the center silicon atom), and an AS_2 mode (out-of-phase motion of adjacent oxygen atoms with respect to the center silicon atom). The observation of AS mode is in agreement with previous reports on oxidized or aged PS [5,11,20], both in spectral profile and peak position. Two small bands at 810 and 456 cm^{-1} are assigned to the symmetric stretching (SS) and rocking (R) modes of the Si–O–Si

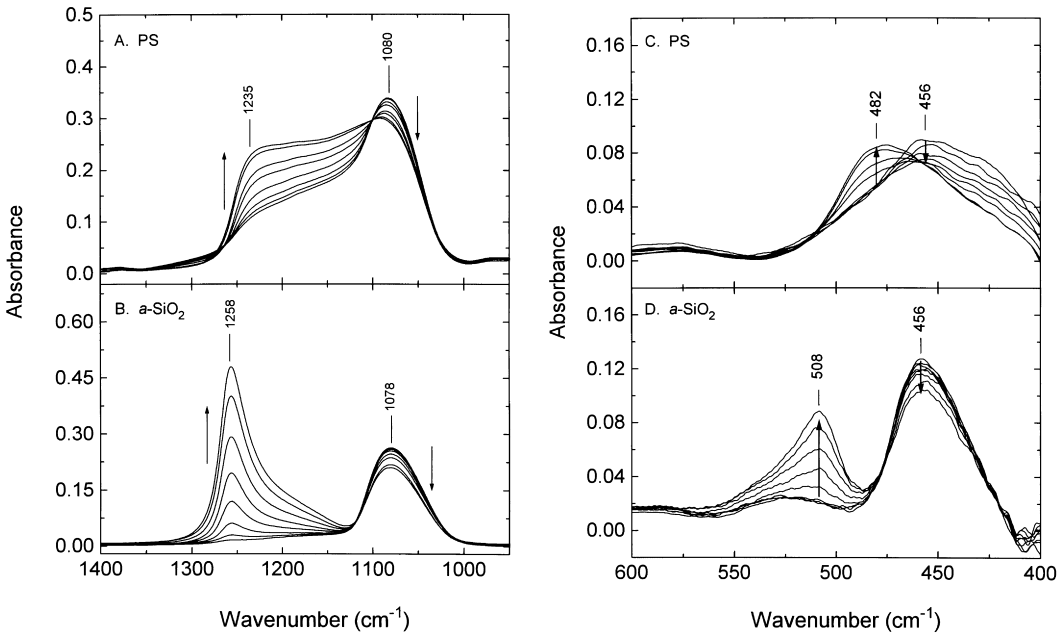

Fig. 4. Polarized FTIR spectra of PS and a-SiO_2 at different oblique angles of incidence: (A) PS in the region of 950–1400 cm^{-1}; (B) a-SiO_2 in the region of 950–1400 cm^{-1}; (C) PS in the region of 400–600 cm^{-1}; and (D) a-SiO_2 in the region of 400–600 cm^{-1}. Arrows show the increase in the oblique angle (0°, 10°, 20°, 30°, 40°, 50°, 60° and 65°).

vibrations. For a-SiO_2 (curve B), the spectrum is in good agreement with previous reports [16,21]. Three major bands at 1078, 810 and 456 cm^{-1} are assigned to the AS_1, SS and R modes of the Si–O–Si entity. Another band at 884 cm^{-1} is observed in PS, and can be attributed to the oxidized hydride deformation mode, $\delta(-O_ySi-H_x)$, as suggested previously [10]. Meanwhile, this band was assigned to the stretching modes of various oxide species, Si_xO_y ($x = 2–4$, $y = 5 - x$) in earlier studies [22,23], as well as a non-hydrogen related origin as suggested in a recent report [8].

In the s-polarized FTIR spectrum of a well-ordered structure, only absorption bands owing to the TO modes should be observed as only TO modes can absorb s-polarized light. The overall similarity of the observed s-polarized FTIR spectra of PS and a-SiO_2 in Fig. 3 gives strong evidence that the observed bands in the PS correspond to the AS_1, SS and R vibrations, similar to those observed in a-SiO_2. The observed differences between the two s-polarized spectra are the following: (a) A relatively higher intensity for the high-energy shoulder of the 1080 cm^{-1} band in PS as compared to the a-SiO_2 film; (b) A new band observed at 884 cm^{-1} in PS; (c) A few bands are observed between the AS mode and the 884 cm^{-1} band in PS; and (d) Band broadening associated with PS (e.g. the broader band over the range 1300–1000 cm^{-1} for the AS mode and the broader band at 456 cm^{-1} for the R mode).

Observations (a)–(c) can be very well understood by referring to the difference in the crystalline structure on the surface of the two materials. The p-polarized spectral feature cannot be observed at normal incidence to the wafer surface for an well-ordered SiO_2 species, as is the case for the a-SiO_2 film. The surfaces of the formed oxides on the tubes and the particles of PS have no well-defined geometric relation to the wafer surface. Many of the tubes have surfaces that have larger and different inclinations with respect to the wafer surface thus allowing the p-polarized (as well as the s-polarized) band to be observed in the s-polarized spectrum. Observation (d) is explained by the larger distribution of the different sizes and shapes of the nanoparticles and nanotubes forming PS.

Table 1
Root mean square (RMS) values for curve-fitting under different band component selection in the 1000–1300 cm^{-1} region for both the p- and s-polarized FTIR spectra of PS and a-SiO_2

Band components in 1300–1000 cm^{-1} range	RMS			
	PS		a-SiO_2	
	p-	s-	p-	s-
2	0.01820	0.01580	0.04790	0.01680
3	0.00694	0.00565	0.02762	0.01121
4	0.00558	0.00298	0.01030	0.00840
5	0.00520	0.00284	0.01010	0.00753

3.2. Polarized FTIR spectra of PS and a-SiO_2

Fig. 4 shows the polarized FTIR spectra of PS and a-SiO_2 at different oblique angles of incidence. For PS, as the angle varies from 0° to 65° off the sample normal, the following changes occur in the high-frequency region (Fig. 4A): (a) A slight blue shift of the 1080 cm^{-1} band; (b) A decrease in its band intensity; and (c) An increase in the intensity of the broad shoulder at higher frequency (1300–1100 cm^{-1}). Fig. 4C depicts the absorption resulting from the Si–O–Si rocking mode. In this region, an apparent band peak at 456 cm^{-1} is observed at $\alpha = 0°$ which shifts to 482 cm^{-1} at $\alpha\alpha = 65°$. There is also a slight change in the band around 810 cm^{-1} (not shown). An attempt to study these changes is made using spectral deconvolution in the next section.

For a-SiO_2, the polarized FTIR results are shown in Fig. 4B and D in the region of 1400–950 cm^{-1} and 600–400 cm^{-1} respectively. As can be seen, a new band appears at 1258 cm^{-1}, and a decrease in the intensity of the band at 1078 cm^{-1} is observed as the oblique angle changes from 0° to 65°. In the low-frequency region, the intensity of the vibrational mode at 456 cm^{-1} decreases whereas that of the mode at 508 cm^{-1} increases. These results are in agreement with previous studies [16].

In the case of PS, we assign the broad band in the high-frequency region (1300–1100 cm^{-1}) to the LO mode of AS_1, as well as to the presence of the AS_2 mode, in-between the AS_1 LO and TO bands in this region. The new band appearing at $\sim$ 482 cm^{-1} and the apparent decrease in the band at $\sim$ 456 cm^{-1} can be attributed to a change in the intensity of the LO and TO modes of the Si–O–Si rocking vibration respectively. These changes are obvious, although the intensities are weaker and the frequency difference is smaller, as compared to those observed for the a-SiO_2 film (Fig. 4D). These results suggest the observation of an LO–TO splitting in the transition from

Table 2
Comparison between the vibration frequencies for TO and LO modes in PS and a-SiO_2 determined by band deconvolution techniques of the polarized FTIR spectroscopy[a]

Oxidized porous silicon (PS)			Amorphous silicon dioxide (a-SiO_2)		
Vibration mode	ν_{peak} (cm^{-1})	$\Delta\nu$	$\Delta\nu$	ν_{peak} (cm^{-1})	Vibration mode
LO (AS_1)	1235	155	180	1258	LO (AS_1)
TO (AS_1)	1080			1078	TO (AS_1)
LO (AS_2)	1138	−45	−60	1160	LO (AS_2)
TO (AS_2)	1183			1220	TO (AS_2)
LO + TO (SS)	810			810	LO + TO (SS)
LO (R)	482	34	52	508	LO(R)
TO (R)	448			456	TO(R)

[a] AS_1: asymmetric stretching mode of Si–O–Si in which adjacent oxygen atoms move in phase; and AS_2 for out of phase; SS: symmetric stretching mode of Si–O–Si; R: rocking mode of oxygen atoms around the Si–Si axis [16]; $\Delta\nu = \nu_{LO} - \nu_{TO}$.

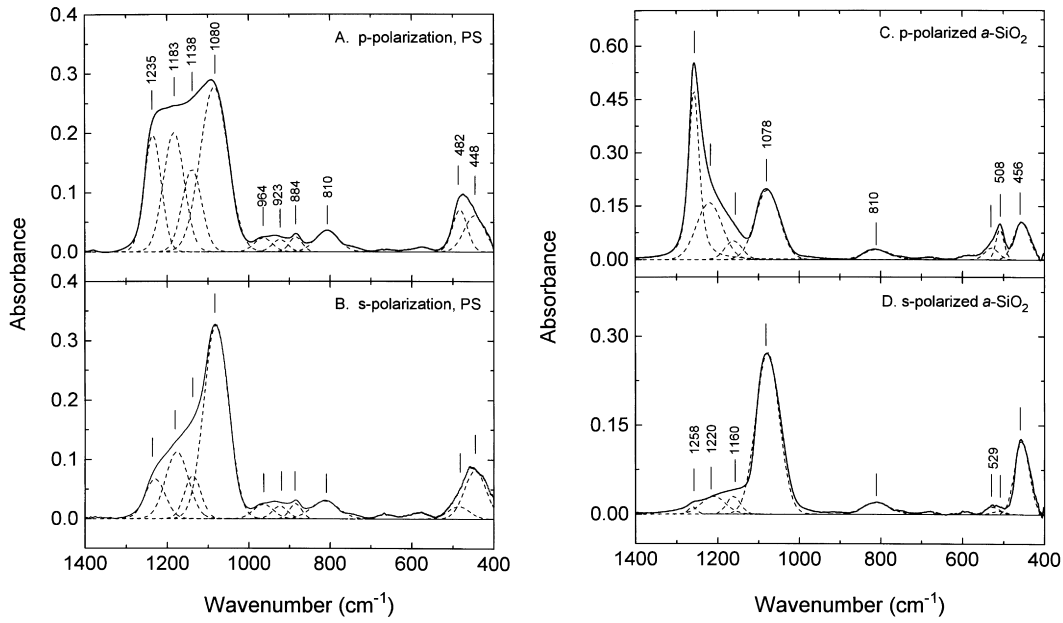

Fig. 5. Curve-fit of the p-polarized and s-polarized FTIR spectra in the region of 400–1400 cm^{-1} for PS and a-SiO_2: (A) The p-polarized spectrum of the PS sample; (B) The s-polarized spectrum of the PS sample; (C) The p-polarized spectrum of the a-SiO_2 sample. A Lorenzian function is chosen for the 1258 cm^{-1} band component owing to a spectral broadening, as also observed previously [16]; and (D) the s-polarized spectrum of the a-SiO_2 sample. Solid lines: Original spectra; Dotted line: deconvoluted band components.

the s- to p-polarization of PS as the oblique angle changes. The LO–TO pair assignment in a-SiO_2 is much easier, as new bands appear at 1258 and 508 cm^{-1} as the oblique angle changes. The vibrational peak pairs at 1259–1076 cm^{-1} (the LO–TO modes of AS_1), and 507–457 cm^{-1} (the LO–TO of the rocking vibration) were reported previously [16]. The clear LO–TO splitting and the large depolarization factor observed in the a-SiO_2 film indicates the effectiveness of the long-range coulombic potential even in the amorphous-like structure. The smaller LO–TO splitting in PS probably indicates less effective long-range interactions. However, the observation of the LO–TO pair suggests that the SiO_x layer in PS still has a short-range ordered structure, probably within the distance of several unit cells.

3.3. Band deconvolution on polarized FTIR spectra

To further support the conclusions we have made regarding the LO–TO frequency assignments in the PS and a-SiO_2 spectra, curve fitting was carried out for both the p- and s-polarized FTIR spectra of both samples in the 1400–400 cm^{-1} region. The best fit is the one that requires the minimum numbers of components with the smallest RMS value. The broad band in the 1300–1000 cm^{-1} region is decomposed into two, three, four and five components for all the polarized spectra, using a Gaussian band shape for each. The RMS values for the selected curve-fitting results are listed in Table 1. It is found that the four-component deconvolution in this region is acceptable as it has the smaller RMS value compared to those with three or fewer band components, also it has the minimum number of components. The assignments of the IR band components to the various Si–O–Si vibrational modes in both PS and a-SiO_2 are summarized in Table 2. These four-component combinations in the 1300–1000 cm^{-1} region and can generally fit the polarized spectra with the oblique angle α changing from 0° to 65°. The results for the p- and s-polarized spectral deconvolution are shown in Fig. 5. No band deconvolution is carried out for the SS vibration mode at 810 cm^{-1} in the present study, as this is a small and broad band centered at 810 cm^{-1} (as also shown previously by Kirk [16]), although Kirk

suggested that it might have an LO (820 cm^{-1})–TO (810 cm^{-1}) splitting in a-SiO_2.

Fig. 5A and B shows the fit for the p- and s-polarized FTIR spectra for PS in the 400–1400 cm^{-1} region. The optimized curve fitting results show that four major bands exist in the 1300–1000 cm^{-1} region for both polarized spectra, with peaks centered at 1080, 1138, 1183 and 1235 cm^{-1} respectively. The two bands around 1138 and 1183 cm^{-1} can be assigned to the LO–TO pair of AS_2, and the band pair at 1235 and 1080 cm^{-1} can be assigned to the LO–TO pair of AS_1, as mentioned earlier. An increase in intensity is observed in the AS_1 LO mode at 1235 cm^{-1} from s- to p-polarization. This change contributes to the broadening and the increase of the shoulder intensity in the 1300–1100 cm^{-1} region. Further, increases in the absorption intensity are observed for both the LO mode at 1138 cm^{-1} and TO mode at 1183 cm^{-1} of AS_2 in the p-polarization direction. All these changes are accompanied by a slight intensity decrease of the TO mode of the AS_1 vibration at 1080 cm^{-1} in the p-polarization direction.

In the low-frequency region from 600 to 400 cm^{-1}, the observed apparent intensity increase and blue shift shown in Fig. 4C can be explained by the results of fitting the spectrum in this region to two bands around 482 and 448 cm^{-1} in both the s- and p-polarization. These are assigned to the LO and TO modes of Si–O–Si rocking vibrations, respectively. It is clear that the spectral changes in this frequency domain upon changing the polarization to p-type, are attributed mostly to the increase in the intensity of the LO mode at 482 cm^{-1}. These changes are small when compared with that observed for the LO mode of the AS vibration (Fig. 4A). The data we show here again indicate that the LO–TO modes splitting can be resolved in p-polarization, and that PS might have LO modes observable even with s-polarization owing to the disorder of the SiO_2 on the surface.

Fig. 5C and D shows the fit for the p- and s-polarized FTIR spectra for a-SiO_2 in the 1400–400 cm^{-1} region. As observed, under p-polarization, the LO and TO modes for the AS_1 vibration are shown at 1258 and 1078 cm^{-1} respectively, whereas the LO and TO modes for the AS_2 vibration are located at 1160 and 1220 cm^{-1} respectively. The frequencies of the AS_2 LO and TO modes are generally in agreement with those of the previous work by Kirk [16]. Under s-polarization, the LO modes for both the AS_1 and AS_2 vibrations can still be observed with low band intensities, in addition to the major TO mode for the AS_1 vibration at 1078 cm^{-1} (Fig. 5D). In both the s- and p-polarized spectra, the presence of a minor band at $\sim$ 529 cm^{-1} should be introduced to account for the apparent shift from s- to p-polarization in this LO vibration mode (Fig. 5C and D), as also shown in Fig. 4D when the oblique angle α changes from 0° to 65°. It seems that this band is not polarized, and is probably because of the intrinsic properties of this material.

4. Discussion

4.1. Vibrational modes of aged PS

Using polarized FTIR spectroscopy combined with band deconvolution techniques, we were able to determine the TO and LO modes of the different vibrations in PS and compare them with those in a-SiO_2 [16]. A comparison between the frequencies of those modes as determined for PS and those in a-SiO_2 is given in Table 2. The important conclusion from this table and Figs. 3–5 can be summarized as follows: (1) There is an apparent increase in the intensity of the LO mode of the AS_1 vibration and the TO mode of the AS_2 vibration in the s-polarized FTIR spectrum of PS. (2) Relatively smaller TO–LO pair splittings are assessed for PS as compared to those observed in a-SiO_2. These differences are discussed in terms of the difference in the structure and thickness of the surface oxide formed on each of the PS nanoparticles and the a-SiO_2 film on the silicon wafer. PS is a three-dimensional inhomogeneous system. However, as we have shown earlier, it maintains a similar spectral feature to a thermally grown a-SiO_2 film that is composed of SiO_4 tetrahedral structure. Evidence for the anisotropic shape of free-standing PS films was shown through scanning electron microscopy (SEM) [24]. The silicon core in PS maintains its original crystalline lattice which is covered by amorphous materials made of SiO_x ($x = 1, 2$) residues. The possible structural difference between PS and a-SiO_2 is the well-ordered SiO_2 feature in the latter, and the disordered feature of the former. Nevertheless, the LO–TO splitting can also be observed in PS, as shown for both the

AS and R vibrations. There is no homogenous composition (in the sense of having long-range translational symmetry for the SiO_4 units) on the surface of PS. In contrast, the a-SiO_2 film shows homogeneity in the oxide film formed on the silicon wafer surface. We discuss the observed differences in more detail later.

Annealed siloxene shows similar FTIR spectrum as oxidized PS [7–9]. However, after annealing, this material can be described as an amorphous, substoichiometric Si : O : H alloy [8]. Therefore, it is quite possible that annealed siloxene and oxidized PS posses similar surface composite, SiO_x. Recently, the importance of the SiO_x surface in PS luminescence mechanism was addressed [14,20].

In agreement with previous results [11], we have also observed two weak absorption bands at $\sim$ 2270 and 3745 cm^{-1} (not shown). They are attributed to the stretching of the Si–H_x group (which has an O atom adjacent to Si), and the stretching of O–H (which has a Si atom adjacent to O) respectively. As the p-type silicon wafer we used is boron doped, the assignment of the 884 cm^{-1} band to the vibration of the B–O–B group cannot be ruled out as the frequencies of ν(BO) and δ(O–B–O) are generally located in the range of 2100–900 and 900–600 cm^{-1} respectively [25]. Other new bands at around 923 and 964 cm^{-1} might be because of the vibrations of the interfacial SiO_x bonds, as these bands are at lower frequency and adjacent to that of the AS mode of Si–O–Si. However, these bands are not so significant in the a-SiO_2 spectrum. Further study is needed to completely assign the origin of these bands.

4.2. Curve-fitting in the region of 1300–1000 cm^{-1}

In general, the Gaussian band shape is assumed, except the 1258 cm^{-1} band component in the case of p-polarized spectrum of a-SiO_2, in which a Lorentzian band shape is used. Asymmetric band shape is not considered in our study. By using symmetric band shape, we were able to fit both the PS and a-SiO_2 IR spectra quite well, as shown in Table 1 and Fig. 5. In these fittings, same or similar bandwidths (with fixed frequency position) are assumed for the same band component appearing in both s- and p-polarized spectra. Slight difference in the bandwidth between the s- and p-polarization might be attributed to the anisotropy in the nature of inhomogeneity.

4.3. Apparent intensity enhancement of AS_2 TO and AS_1 LO modes in PS

If we compare the IR band in 1300–1000 cm^{-1} region for PS and a-SiO_2, two possibilities are suggested for the origin of the broadening and relatively high absorption intensity of the AS_1 LO mode and the AS_2 TO mode, even in the s-polarized FTIR spectrum of PS. The LO mode should be p-polarized with its moment perpendicular to the wafer surface and thus its absorption should not be observed in the s-polarized spectrum. This will be true if the surface of the oxide formed is parallel to that of the wafer. First, we explain this apparent enhancement as a result of the structural disorder in PS. Owing to the porous structure of PS, the columns can be formed [25] with their surface planes having many different orientations with respect to the wafer surface plane. Thus the moment of the LO modes could be oriented at different angles from the wafer surface plane. This leads to absorption by the LO modes even when the electric field of the light is parallel to the wafer surface, e.g. the s-polarized spectrum. This results in the observed apparent enhancement of the absorption in this region.

There is yet another possibility that could result in an increase in the AS_2 modes owing to mechanical coupling with the intense AS_1 mode [16]. The coupling results from the electrostatic interaction in a spatially confined and disordered system [26], as observed in silicon nanocrystal powders prepared by a different method [27]. In fact, this is the effect of electron–phonon coupling enhancement owing to the Frohlich interaction [28]. Kirk [16] reported possible mixing between the AS_1 and AS_2 modes when he compared the results for a-SiO_2 with crystalline a-quartz. In his work, a decrease in the absorption strength of the AS_1 mode (1256 cm^{-1} for LO and 1076 cm^{-1} for TO), and a concomitant increase in the oscillator strength of the AS_2 mode (at 1160 cm^{-1} for LO and at 1200 cm^{-1} for TO) were observed. As was shown by Kirk [16], it is the repulsion between the AS_1 and AS_2 vibrational levels that leads to the AS_2 LO–TO band inversion in their frequency position in a-SiO_2 IR spectrum. Similar band inversion is observed in the PS spectrum in the present study. As the SiO_x on the PS surface is expected to be more disordered, such a coupling

could be stronger owing to the relaxation of symmetry restrictions and thus lead to a larger enhancement of the AS_2 type bands than that observed in a-SiO_2.

4.4. Comparison origin of the LO–TO splitting in PS and a-SiO_2

In general, the long-range coulombic interaction between the different moments of the different vibrations of the Si–O–Si unit cell is the origin of the LO–TO splitting. The stronger the interaction, the larger the splitting. Typically this is the case for ordered crystalline materials. It is also observed in amorphous materials such as a-SiO_2 by taking a proper average over a proper distribution as discussed in a previous study [16]. The LO–TO mode splitting of the AS_1 vibration in PS is $\sim$155 cm^{-1}, whereas that in a-SiO_2, $\sim$180 cm^{-1}, is observed in present study ($\sim$178 cm^{-1} in Kirk's work) [16]. The decrease in the observed splitting in PS (as compared to a-SiO_2) is owing to disorder-induced effects, which are quite common in vitreous SiO_2 [15,29], vitreous GeO_2, and BeF_2 [15], as well as in ν-As_2O_3, and ν-As_2S_3 [30]. The decrease in the splitting arises from the broader distribution that has to be used in calculating the average frequencies in these inhomogenous materials. The structural inhomogeneity in the PS is revealed by the observed vibrational band broadening, the absorption enhancement of the forbidden vibrations and the depolarization of the absorption spectrum. Our results also suggest that as the disorder and confinement become stronger, the LO phonon–electron coupling also becomes stronger [28], which may be the cause of vibrational and electronic transition variations of PS. This can be seen from the comparison of the LO mode intensity of the AS_1, AS_2, SS, and R vibrations of PS.

5. Conclusion

The similarities and differences between aged luminescent PS film and non-luminescent a-SiO_2 film formed on Si (100) surface, were discussed in terms of the LO and TO vibrational modes. A possible assignment of the LO–TO pairs for the various vibrational modes of the SiO_x group in solid PS was made using curve-fitting of the s- and p-polarized FTIR spectra. The IR band broadening in the 1300–1100 cm^{-1} region, the apparent enhancement of the AS_2 vibrations in the s-polarized spectrum, the lower polarization ratios, and the smaller LO–TO pair splitting in PS as compared to an a-SiO_2 film, are all associated with the much greater disorder of the PS oxidized surface.

The results given earlier support a mechanism [31] in which the emission of aged PS is proposed to originate from oxidized disordered surface sites. This inhomogeneously broadened distribution of the sites on the oxidized surface could be owing to either physical or chemical defects of this highly disordered surface.

Acknowledgements

The authors would like to acknowledge Professor J.L. Gole of Georgia Institute of Technology for helpful discussions, and Dr. Z. Zhang, Dr. Q. Chen, and Mr. C. Liu of Georgia Institute of Technology for their assistance in preparing the thermally oxidized silicon wafer. The authors would like to thank the Office of Naval Research (Grant No. N00014-95-1-0306). B. Zou acknowledges the partial support of this project of the Georgia Tech Molecular Design Institute supported by the Office of Naval Research (Contract N00014-95-1-1116).

References

[1] L.T. Canham, Appl. Phys. Lett. 57 (1990) 1046.
[2] L. Brus, J. Phys. Chem. 98 (1994) 3575.
[3] T. Nakamura, H. Omyoya, K. Sasaki, N. Azuma, H. Mimura, Appl. Surf. Sci. 113/114 (1997) 145.
[4] P.M. Fauchet, L. Tsybeskov, Ju.V. Vandyshev, A. Dubois, C. Peng, Proc. SPIE 2141 (1994) 155.
[5] Y.H. Xie, W.L. Wilson, F.M. Ross, J.A. Mucha, E.A. Fitzgerald, J.M. Macaulay, T.D. Harris, J. Appl. Phys. 71 (1992) 2403.
[6] M.A. Hory, R. Herino, M. Ligeon, F. Muller, F. Gaspard, I. Milhalcescu, J.C. Vial, Thin Solid Films 255 (1995) 200.
[7] M.S. Brandt, H.D. Fuchs, M. Stutzman, J. Weber, M. Cardona, Solid State Commun. 81 (1992) 307.
[8] M. Stutzmann, M.S. Brandt, M. Rosenbauer, H.D. Fuchs, S. Finkbeiner, J. Weber, P. Deak, J. Lumin. 57 (1993) 321.
[9] M.A. Tischer, R.T. Collins, Solid State Commun. 84 (1992) 819.
[10] V.M. Dubin, F. Ozanam, J.N. Chazalviel, Thin Solid Films 255 (1995) 87.
[11] D.B. Mawhinney, J.A. Glass Jr., J.T. Yates Jr., J. Phys. Chem. B 101 (1997) 1202.
[12] J.L. Gole, D.A. Dixon, J. Phys. Chem. B 101 (1997) 8098.

[13] J.L. Gole, F.P. Dudel, D. Grantier, D.A. Dixon, Phys. Rev. B 56 (1997) 2137.
[14] Y. Kanemitsu, S. Okamoto, M. Otobe, S. Oda, Phys. Rev. B 55 (1997) R7375.
[15] F.L. Galeener, A.J. Leadbetter, M.W. Stringfellow, Phys. Rev. B 27 (1983) 1052.
[16] C.T. Kirk, Phys. Rev. B 38 (1988) 1255.
[17] A. Pasquarello, R. Car, Phys. Rev. Lett. 79 (1997) 1766.
[18] L. Song, M.A. El-Sayed, P.C. Chen, J. Appl. Phys. 82 (1997) 836.
[19] S.M. Prokes, Porous silicon nanostructures, in: A.S. Edelstein, R.C. Cammarata (Eds.), Nanomaterials: Synthesis, Properties and Applications, Institute of Physics, Bristol, 1996 Chapter 7.
[20] Y. Kanemitsu, S. Okamoto, Phys. Rev. B 56 (1997) R1696.
[21] M. Trchova, J. Zemek, K. Jurek, J. Appl. Phys. 82 (1997) 3519.
[22] T. Unagami, Jpn. J. Appl. Phys. 19 (1980) 231.
[23] M. Nakamura, Y. Mochizuki, K. Usami, Y. Itoh, T. Nozaki, Solid State Commun. 50 (1984) 1079.
[24] A. Bruska, E.V. Astrova, U. Falke, T. Raschke, T. Radehaus, Ch. Hietschold, Thin Solid Films 297 (1997) 79.
[15] K. Nakamoto, Infrared and Raman spectra of Inorganic and Coordination Compounds, 3, Wiley-Interscience, New York, 1978.
[26] M.H. Degani, G.A. Farias, Phys. Rev. B 42 (1990) 11 950.
[27] S.-T. Li, S.J. Silvers, M.S. El-Shall, J. Phys. Chem. B 101 (1997) 1794.
[28] T. Takagahara, Ultrafast inter-subband relaxation of photoexcited carriers in semi-conductor quantum dots, in: T. Yajima, K. Yoshihara, C.B. Harris, S. Shionoya (Eds.), Ultrafast Phenomena VI, 48, Springer, Berlin, 1988.
[29] R.M. Almeida, Phys. Rev. B 45 (1992) 161.
[30] F.L. Galeener, G. Lucovsky, R.H. Geils, Phys. Rev. B 19 (1979) 4251.
[31] J.-P. Wang, L. Song, B.-S. Zou, M.A. El-Sayed, Phys. Rev. B, in press.